Supporting Information for Publication

Droplet Manipulation on Wettable Gradient Surfaces with Micro-/Nano-Hierarchical Structure

Yong P. Hou,[‡] Shi L. Feng,[‡] Li M. Dai,*,[§] and Yong M. Zheng*,[‡]

[‡] Key Laboratory of Bio-Inspired Smart Interfacial Science and Technology of Ministry of Education, School of Chemistry and Environment, Beihang University, Beijing, 100191 (P. R. China)

[§]Center of Advanced Science and Engineering for Carbon, Department of Macromolecular Science and Engineering, Case Western Reserve University, Cleveland, OH 44106 (USA)

E-mail: zhengym@buaa.edu.cn, liming.dai@case.edu.

Content：
EXPERIMENTAL SECTION

Preparation of wettable gradient surface on stainless steel mesh. Stainless steel mesh (size of 2 × 0.5 cm, pore diameters of 35 μm) was consecutively rinsed in ethanol and deionized water under ultrasonction for 5 min each to remove impurities. Thereafter, the treated mesh was perpendicularly inserted into an aqueous solution of electrolyte ($CuNO_3 \cdot 6H_2O$, 0.05 M) and treated with cathodic electrodeposition by using a narrow-strip Cu foil (size of 2 × 0.5 cm) as an anode and the distance between cathode and anode is 0.5 cm. Due to the different resistances between different areas on the mesh and the anode, the current gradient was formed during the electrodeposition process. A drain at the bottom of the chamber was used to control the electrodeposition time (see Figure 1a). By so doing, the current gradient and time gradient were used to form the wettable gradient. The specimens thus were cleaned thoroughly with deionized water and dried ($70^{o}C$, 3 min) prior to subsequent analyses.

Characterization. Water contact angles (CAs) on gradient surfaces were measured by the optical contact angle meter system (OCA40Micro, Dataphysics Instruments GmbH, Germany). The volume of a droplet was 5 μL and the static CA was measured for five times. The movement behaviour of droplets (10 μL) on wettable gradient surfaces was recorded by CCD camera. The microstructure of the stainless steel mesh was observed by scanning electron microscope (SEM) (JSM-7500F, JEOL, Japan) with a voltage of 10 kV. X-ray diffraction (XRD) analyses were performed on XRD-6000 (Shimadzu, Japan). X-ray photoelectron spectroscopic (XPS) measurements were made on an ESCALAB 250 instrument (Thermo Fisher Scientific, USA). We used the origin 8.6 software to analyze the relationship between CA and ACA, RCA via Linear equation.

Supplementary Figure Legends: Figure S1-S6
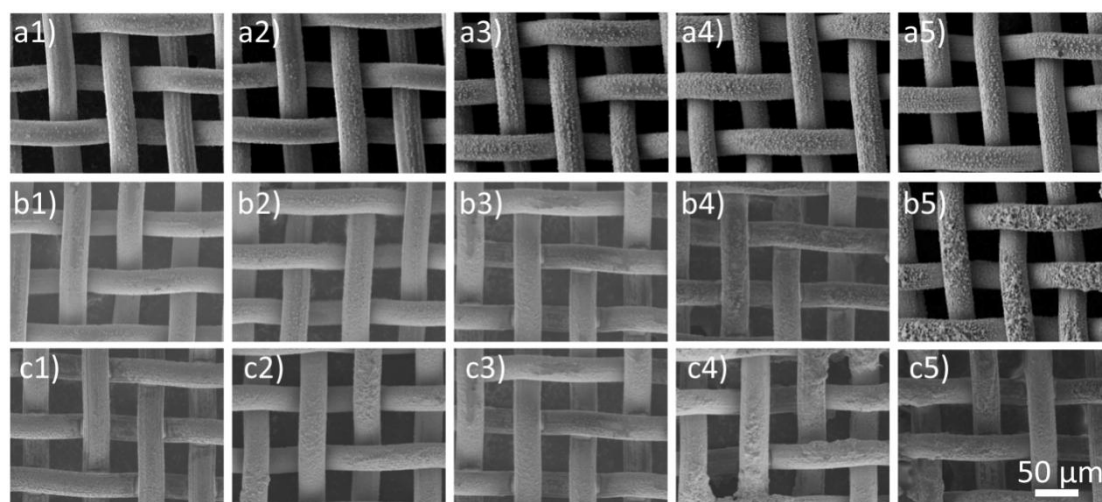
Figure S1

Figure S1. SEM photos of the deposition structure on different position (distance to the top edge of mesh) of different samples. a1-a5) Sample-A, 4 mm, 7 mm, 10 mm, 13 mm, 16 mm, respectively. b1-b5) Sample-B, 4 mm, 7 mm, 10 mm, 13 mm, 16 mm, respectively. c1-c5) Sample-C, 4 mm, 7 mm, 10 mm, 13 mm, 16 mm, respectively.
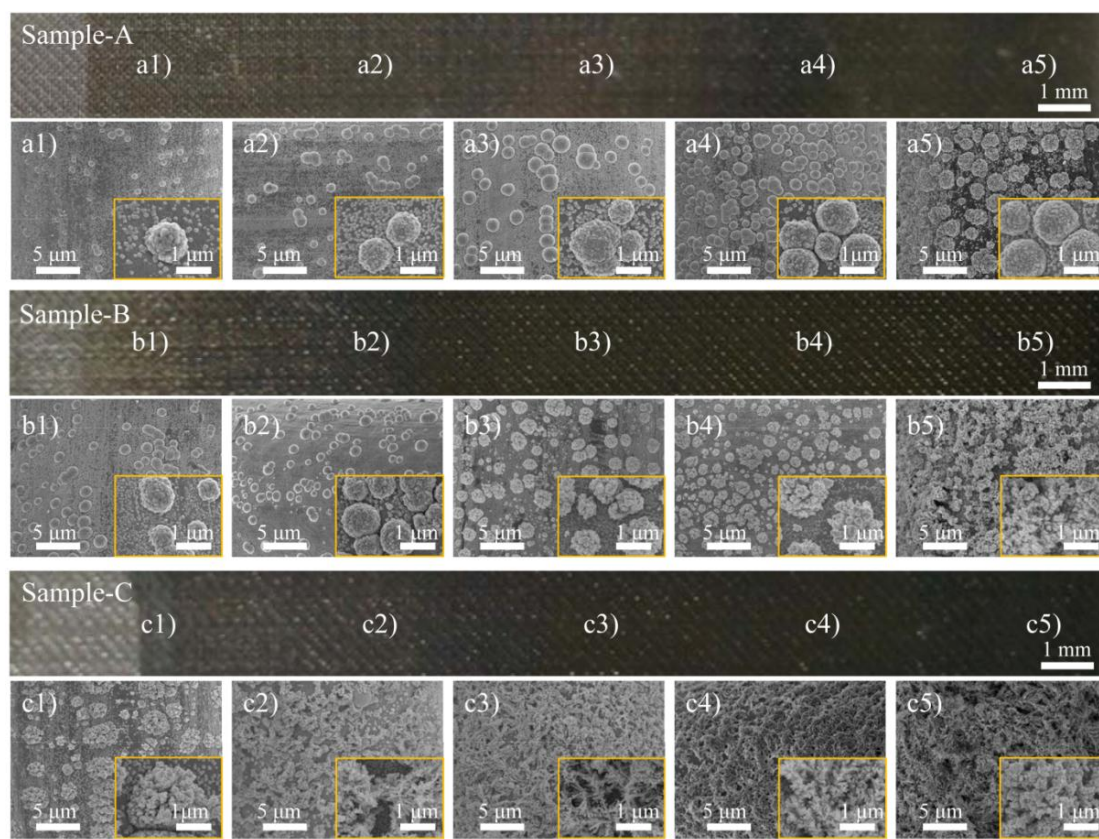
Figure S2

Figure S2. SEM photos of the deposition structure on different position (distance to the top edge of stainless steel mesh) of different samples. a1-a5) Sample-A, 4 mm, 7 mm, 10 mm, 13 mm, 16 mm, respectively. b1-b5) Sample-B, 4 mm, 7 mm, 10 mm, 13 mm, 16 mm, respectively. c1-c5) Sample-C, 4 mm, 7 mm, 10 mm, 13 mm, 16 mm, respectively.
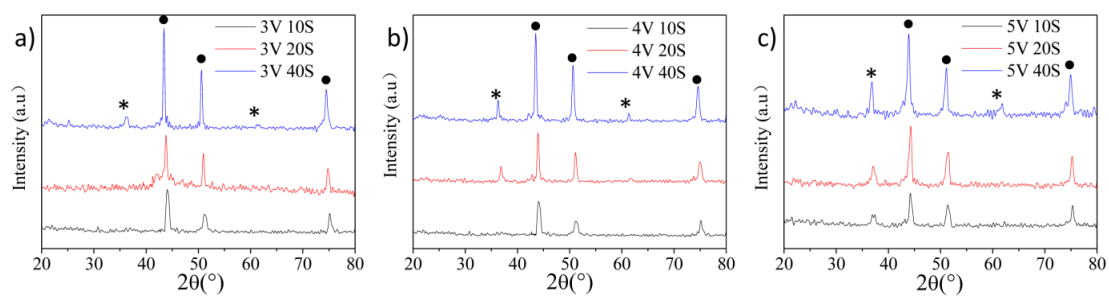
Figure S3

Figure S3. X-ray diffraction (XRD) profiles of different samples prepared at different conditions (10 s, 20 s, 40 s correspond to the deposition time of the area a2, a3, a5 of Sample-A or the area b2, b3, b5 of Sample-B or the area c2, c3, c5 of Sample-C, respectively). The diffraction peaks marked with solid circles attribute the Cu substrates (JCPDS. 85-1326). For a long deposition time or at a high voltage (3 V for 40 s; 4 V for 20 or 40 s; 5 V for 10 or 20 or 40 s), small cuprous oxide (Cu_2O) peaks (*) are observed (JCPDS. 78-2076), which provide a clear evidence for the formation of Cu_2O.
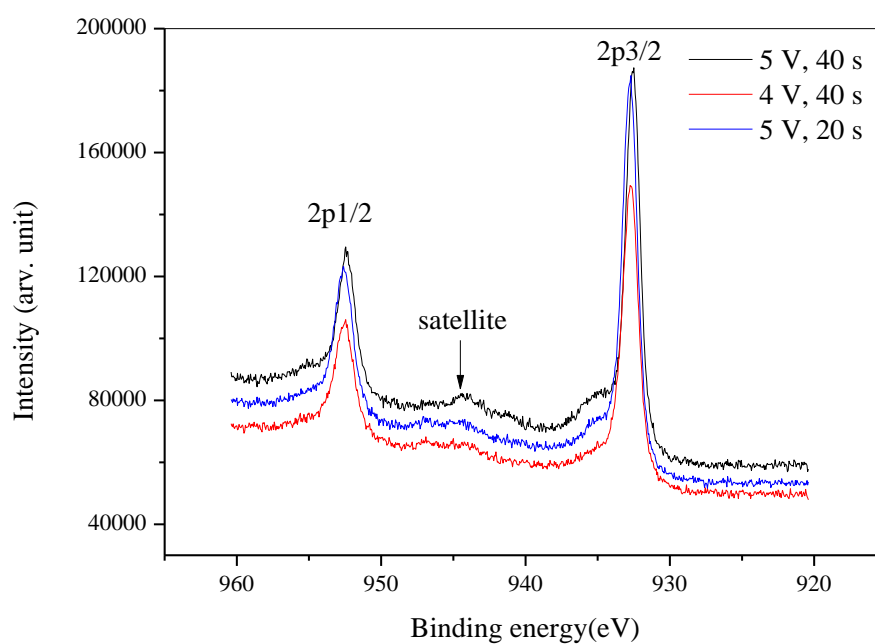
Figure S4

Figure S4. High-resolution XPS spectra of different samples prepared at different conditions. The most important character is the shakeup satellite, indicating the presence of cupric oxide (CuO). Both XRD and XPS results indicate cuprous oxide (Cu_2O) and CuO formed on the copper surface at a high voltage or for a long electrodeposition time, which is probably resulted from oxidation reaction between the copper and oxygen in the electrolyte. The absence of CuO peak in XRD spectrum may be due to the amorphous structure of CuO.
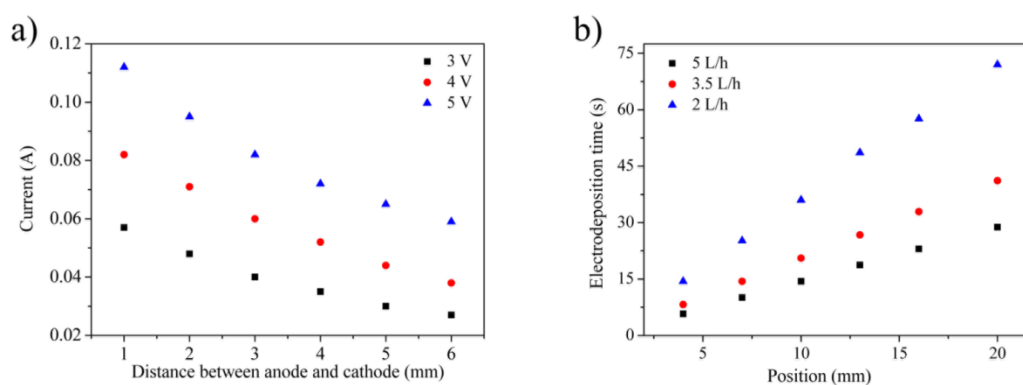
Figure S5

Figure S5. a) The influence of the distance between anode and cathode on current at different voltages. b) Electrodeposition time at different position under different flow velocity of electrolyte. Clearly, the current and treatment time could be adjusted by the distance between anode and cathode or and flow velocity of electrolyte, respectively.
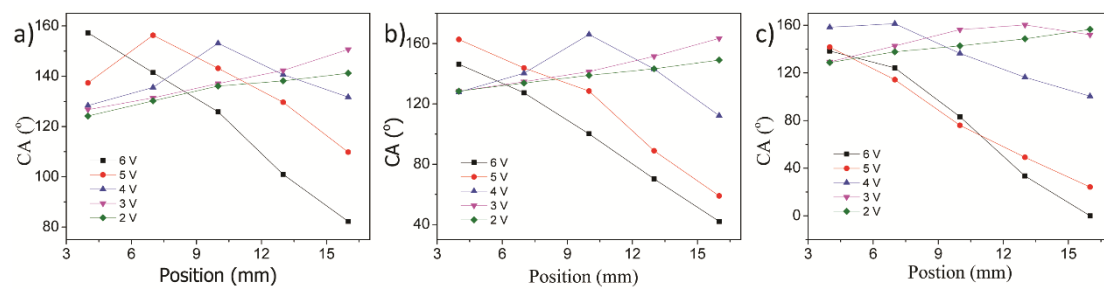
Figure S6

Figure S6. Contact angle (CA) on different position of stainless steel mesh treated by cathodic electrodeposition under different voltage and flow velocity. a) 5 L/h. b) 3.5 L/h. c) 2 L/h.
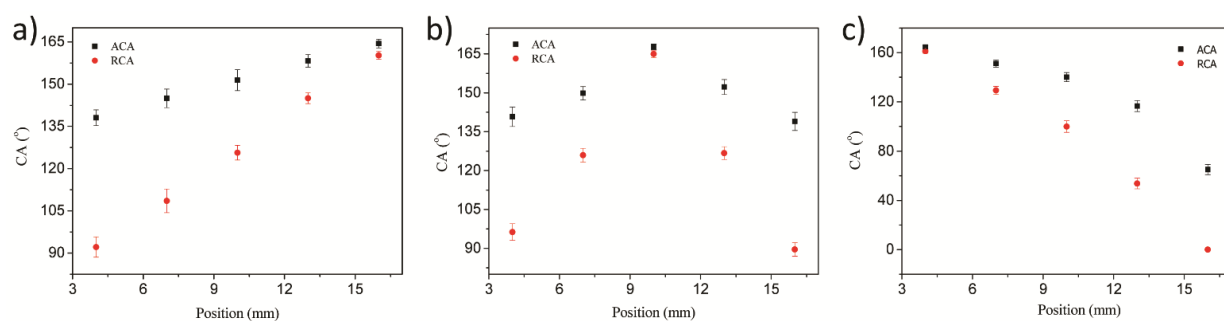
Figure S7. Advancing contact angle (ACA) and receding contact angle (RCA) on different sample surfaces. a) Sample-A. b) Sample-B. c) Sample-C.
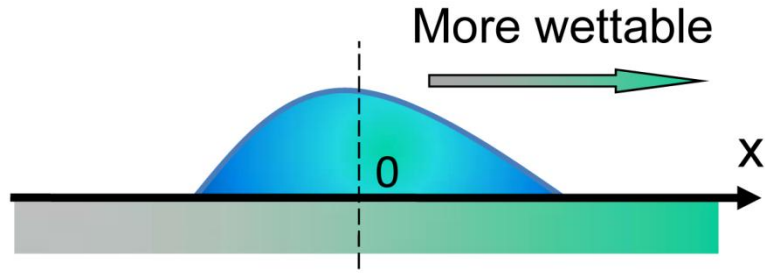
Figure S8. Plan view of the footprint of the water droplet sited on the wettability gradient surface. When a droplet is contact with a wettability gradient surface, the two fronts along the wettability gradient axis have different CAs. The dynamic CAs of the moving drop are, to a good approximation, equal to the Young CA in the middle of the drop base. The wettability gradient force could be described as:

$$F_w = \pi \gamma R^2 k \frac{d \cos \theta}{dx} = \pi \gamma R^2 \frac{d \cos \theta}{d\theta} \frac{d\theta}{dx} = \pi \gamma R^2 k \sin \theta$$

in which R is the base radius of the droplet, γ is the surface tension of water, θ is the position-responsive sessile CA of the water droplet, dx is the integrating variable along the wettability gradient, and k is the wettability gradient (equal to dθ/dx).